

Fabrication of a novel organic-inorganic hybrid nanocatalyst and its application for the synthesis of bis(pyrazolyl)methanes

Abdolkarim Zare*^a, Mojtaba Oraki^a

a) Department of Chemistry, Payame Noor University, PO Box 19395-3697, Tehran, Iran

Received 9 April 2023; received in revised form 30 June 2023; accepted 31 June 2023 (DOI: 10.30495/IJC.2023.1983633.2003)

ABSTRACT

A novel organic-inorganic hybrid nanomaterial was fabricated by anchoring an organic constituent possessing a 4,4'-bipyridine framework to nano-silica (as an inorganic constituent). The nanomaterial, namely 1-(Si-pr)-[4,4'-bipyridine]-1,1'-dium dihydrogen phosphate anchored to nano-silica (SPBDS), was characterized by EDS, elemental mapping, FE-SEM, FT-IR, XRD, and TG analyses. Thereafter, bis(pyrazolyl)methanes were successfully constructed through the solvent-free reaction of 3-methyl-1-phenyl-1*H*-pyrazol-5(4*H*)-one (2 eq.) and aryl aldehydes (1 eq.) using SPBDS. The catalyst was reusable nine times without a significant decrement in its performance.

Keywords: *Organic-inorganic hybrid nanocatalyst, 1-(Si-pr)-[4,4'-bipyridine]-1,1'-dium dihydrogen phosphate anchored to nano-silica (SPBDS), Bis(pyrazolyl)methane, Solvent-free*

1. Introduction

A practical and helpful approach toward the fabrication of organic-inorganic hybrid nanomaterials is anchoring an organic constituent to nanostructured inorganic supports. Characteristics of these materials depend on a combination of their organic and inorganic constituents properties and the ratio of each constituent. Some benefits of hybrid nanomaterials involve enhanced activity and performance, proper steadiness (thermal and chemical), ecofriendly nature, easy operation and separation, flexible design, and possessing a wide range of applications [1-19]. Besides, in the catalysis field, they simultaneously have the properties of heterogeneous and homogeneous catalysts [2-11]. Organic-inorganic hybrid nanomaterials have been applied for the treatment of colon cancer [12], Lu(III) adsorption [13], and monitoring drug delivery [14]. They have also been utilized in biomembrane vesicles [15], lithium batteries [16], transistors [17], supercapacitors [18], and chemotherapy [19]. The Solvent-free technique is a beneficial, practical, efficacious, and eco-friendly approach which have been

widely used for the construction of diverse organic compounds; its privileges have been documented in the literature [20-23].

Pyrazole framework is an important constituent of many bioactive, medicinal and, industrial compounds [24-34]; for instance, rimonabant is used to treat obesity, fomepizole inhibits alcohol dehydrogenase, and celecoxib has anti-inflammatory activity (**Fig. 1**) [24,25].

Furthermore, numerous biological activities have been reported for pyrazole-bearing compounds, e.g., anticancer [26], antioxidant [27], growth inhibitors of phytopathogenic fungi [28], anti-tubercular [29], and α -glucosidase inhibitory [30]. They have been also utilized in chemosensors [31], fluorescence probes [32], as corrosion inhibitors [33], and complexing agents [34].

A category of compounds having a pyrazole framework is bis(pyrazolyl)methanes, which could be constructed by the reaction of 3-methyl-1-phenyl-1*H*-pyrazol-5(4*H*)-one (2 eq.) and aryl aldehydes (1 eq.) using a catalyst [35-44].

*Corresponding author:

E-mail address: abdolkarimzare@pnu.ac.ir;
abdolkarimzare@yahoo.com (A. Zare);

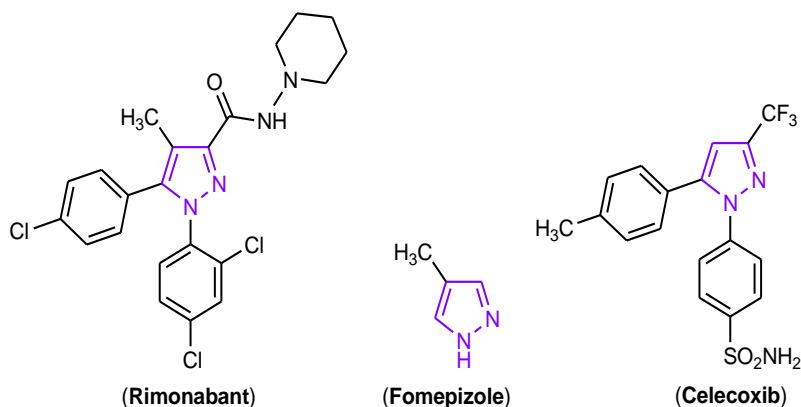


Fig. 1. The drugs containing pyrazole scaffold.

Having the above issues in mind, developing a novel organic-inorganic hybrid nanocatalyst for the construction of bis(pyrazolyl)methanes can be valuable. Herein, we have developed 1-(Si-pr)-[4,4'-bipyridine]-1,1'-dium dihydrogen phosphate anchored to nano-silica (SPBDS) to promote the construction of bis(pyrazolyl)methanes.

2. Experimental

2.1. Materials and instruments

Information on materials and instruments have been reported in supplementary information.

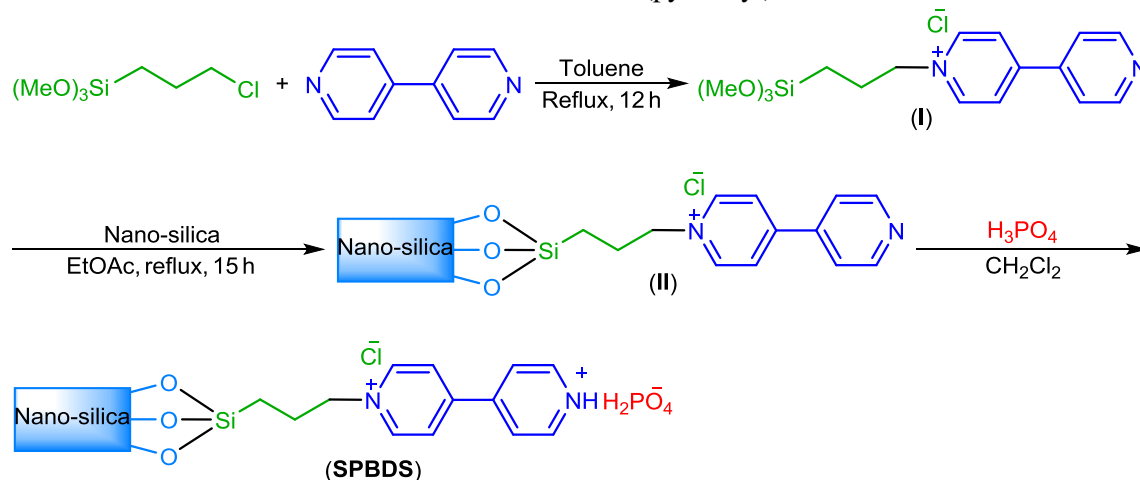
2.2. Fabrication of SPBDS

A mixture of (3-chloropropyl)trimethoxysilane (5 mmol, 0.994 g) and 4,4'-bipyridine (5 mmol, 0.781 g) in toluene (15 mL) was stirred for 12 h under reflux conditions; thereafter, the solvent was distilled under vacuum at 95 °C to produce **I**. In continue, nano-silica (10 mmol, 0.600 g) and compound **I** were refluxed and stirred in EtOAc (15 mL) for 15 h to give **II**. Lastly, H_3PO_4 (5 mmol) was added slowly to **II** in CH_2Cl_2 (10

mL) at room temperature and stirred for 6 h at the same temperature and 2 h under reflux conditions to provide SPBDS (**Scheme 1**). Before each step (the fabrication of **II** and SPBDS), an ultrasound wave was irradiated into the reaction mixture to disperse it. Moreover, **II** and SPBDS were separated from their reaction mixtures by centrifuging and decanting, washed with the solvent used in that step, and dried.

2.3. General procedure for the construction of bis(pyrazolyl)methanes

3-Methyl-1-phenyl-1*H*-pyrazol-5(4*H*)-one (1 mmol, 0.174 g), aldehyde (0.5 mmol), and SPBDS (0.03 g) were added in a reaction vessel, and the mixture was stirred by a rod at 80 °C. When TLC indicated consuming the reactants, the reaction mixture was cooled to ambient temperature, EtOAc (15 mL) was added, and stirred under reflux conditions for 2 min, followed by centrifuging and decanting to separate SPBDS; it was washed by EtOAc (2×3 mL), dried and used for next run. The acquired solution after the decanting was distilled, and the solid residue was recrystallized from EtOH (95%) to construct the pure bis(pyrazolyl)methane.



Scheme 1. The fabrication of SPBDS.

Note: Selected spectral data and original spectrums of bis(pyrazolyl)methanes have been reported in the supplementary information.

3. Results and Discussion

3.1. Characterization of SPBDS

1-(Si-pr)-[4,4'-bipyridine]-1,1'-dium dihydrogen phosphate anchored to nano-silica (SPBDS) was fabricated through the nucleophilic substitution reaction of 4,4'-bipyridine and (3-chloropropyl)trimethoxysilane, subsequently, anchoring the obtained compound to nano-silica, and finally, addition of H_3PO_4 (**Scheme 1**). It was characterized by EDS (energy-dispersive X-ray spectroscopy), elemental mapping, FE-SEM (field emission scanning electron microscopy), FT-IR, XRD (X-ray diffraction), and TG (thermal gravimetric) analyses.

The EDS analysis (**Fig. 2**) and elemental mapping images (**Fig. 3**) indicated Si, which is belong to the inorganic constituent of SPBDS (i.e., nano-silica) and Si-pr moiety. The analyses showed O, which is related to the nano- SiO_2 and the $H_2PO_4^-$. The EDS analysis

indicated the peak related to C of the alkyl chain and [4,4'-bipyridine]-1,1'-dium component; the elemental mapping analysis was also showed this element. Presence of the N related to [4,4'-bipyridine]-1,1'-dium was verified by both analyses. Existing $H_2PO_4^-$ in the structure of SPBDS was confirmed by observing P in the EDS and elemental mapping analyses. Furthermore, well distribution of the elements in the surface of SPBDS was seen in the elemental mapping images.

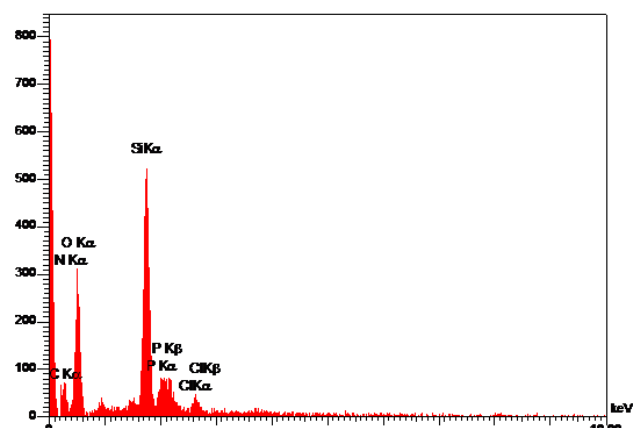


Fig. 2. The EDS spectrum of SPBDS.

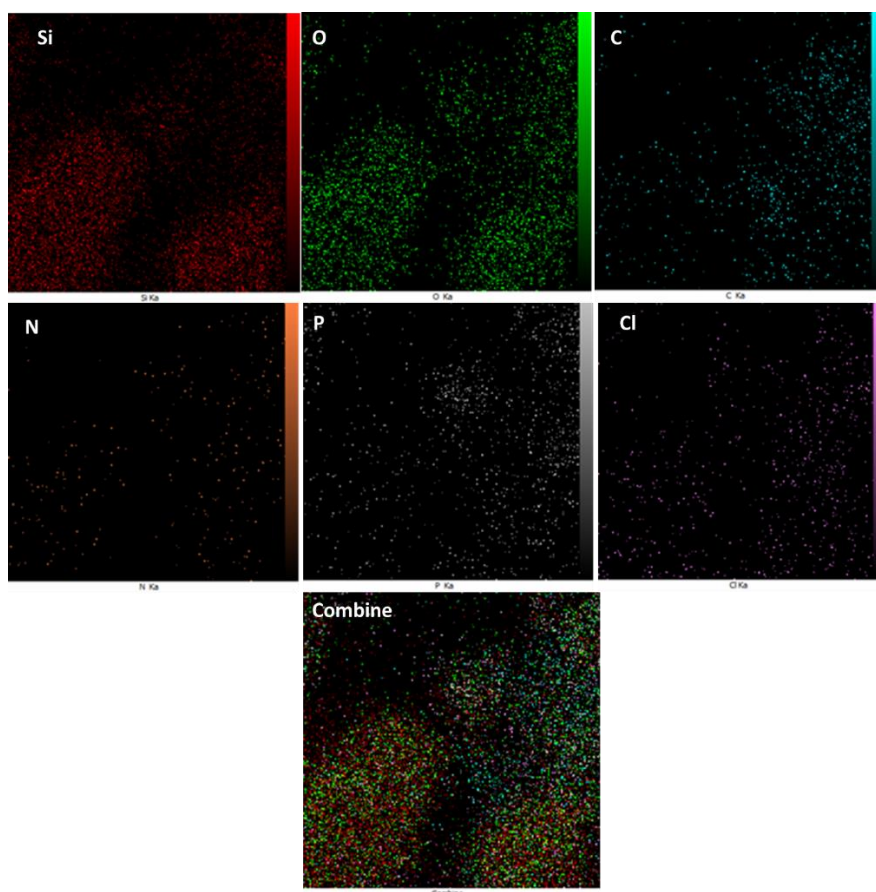


Fig. 3. The elemental mapping images of SPBDS.

Morphologies and sizes of the particles were specified by FE-SEM pictures (**Fig. 4**). As the pictures show, particles of SPBDS have diverse crystalline shapes, and they are in the range of nanoscale (e.g., 11.35, 15.23, and 18.36 nm).

The successful fabrication of 1-(Si-pr)-[4,4'-bipyridine]-1,1'-dium dihydrogen phosphate anchored to nano-silica was also proved by observing the peaks related to all functional groups and bonds of it in the FT-IR spectrum (**Fig. 5**). The peak that appeared at 473 cm^{-1} is ascribed to Si-O bond (rocking). The peaks pertained to symmetric and asymmetric stretching

vibrations of Si-O-Si were observed at 797 and 1096 cm^{-1} , correspondingly. The peak appeared at 1432 cm^{-1} is corresponded to aromatic C=C bonds. The peak at 1578 cm^{-1} is attributed to C=N bonds of [4,4'-bipyridine]-1,1'-dium constituent. C-H bonds of Si-pr moiety gave peaks at 2936 and 2979 cm^{-1} . Bending and stretching vibrations of aromatic C-H bonds gave peaks at 1009 and 3080 cm^{-1} , respectively. The broad peak observed at $\sim 2530\text{-}3730\text{ cm}^{-1}$ is ascribed to OH groups of H_2PO_4^- and adsorbed H_2O on the silica surface.

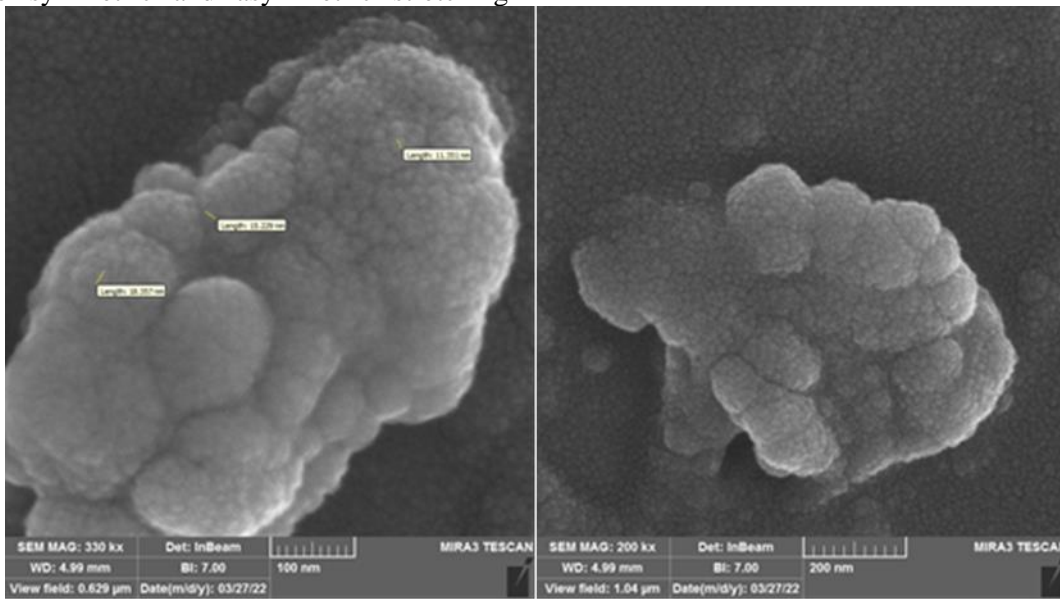


Fig. 4. The FE-SEM image of SPBDS.

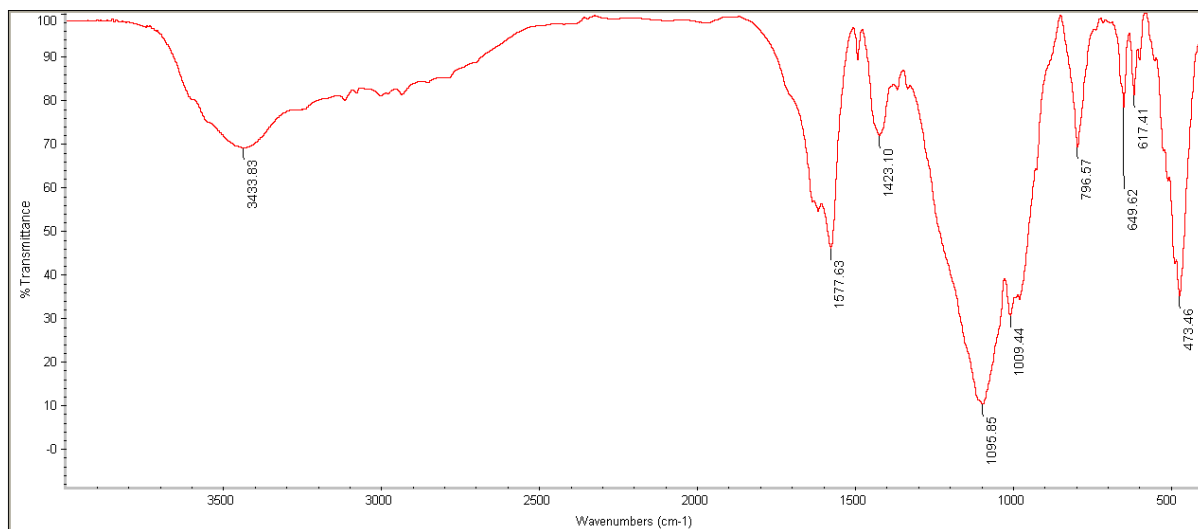


Fig. 5. The FT-IR spectrum of the nanomaterial.

Fig. 6 indicates the XRD pattern of 1-(Si-pr)-[4,4'-bipyridine]-1,1'-dium dihydrogen phosphate anchored to nano-silica in a domain of $2\theta = 10\text{--}80^\circ$. The Presence of the amorphous form of silica was confirmed by observation of a broad peak at $2\theta \approx 13.70\text{--}37.80^\circ$. The sharp diffraction lines showed in **Table 1** can be related to the diverse crystalline shapes of the nanomaterial, which formed due to anchoring the organic constituent to nano-silica. Additionally, full width at half maximum (FWHM), interplanar distance, relative intensity of the diffraction lines, and particle sizes of SPBDS are given in **Table 1**. Debye–Scherrer equation ($D = K\lambda/(\beta\cos \theta)$) was used for the calculation of the particles sizes (D); K is the shape factor (0.9), λ is Cu radiation wavelength (0.154178 nm), and β is FWHM in radian. The

calculated particles sizes of SPBDS were in the range of 6.77–41.80 nm, which were in good agreement with the sizes attained from the FE-SEM pictures (**Fig. 4**).

Thermal gravimetric analysis of SPBDS was achieved at a range of 25 to 600 °C; the relevant diagram is depicted in **Fig. 7**. The first weight loss (up to $\sim 180^\circ\text{C}$) can be attributed to the loss of physically adsorbed water and other solvents on the nanomaterial surface. The other weight losses (at $\sim 180\text{--}300$ and $\sim 300\text{--}600^\circ\text{C}$) can be related to the decomposition of 1-(Si-pr)-[4,4'-bipyridine]-1,1'-dium moiety and the condensation of the silanol groups. These data verified the successful grafting of the organic motif on the nano-silica surface, and the suitable thermal stability of SPBDS.

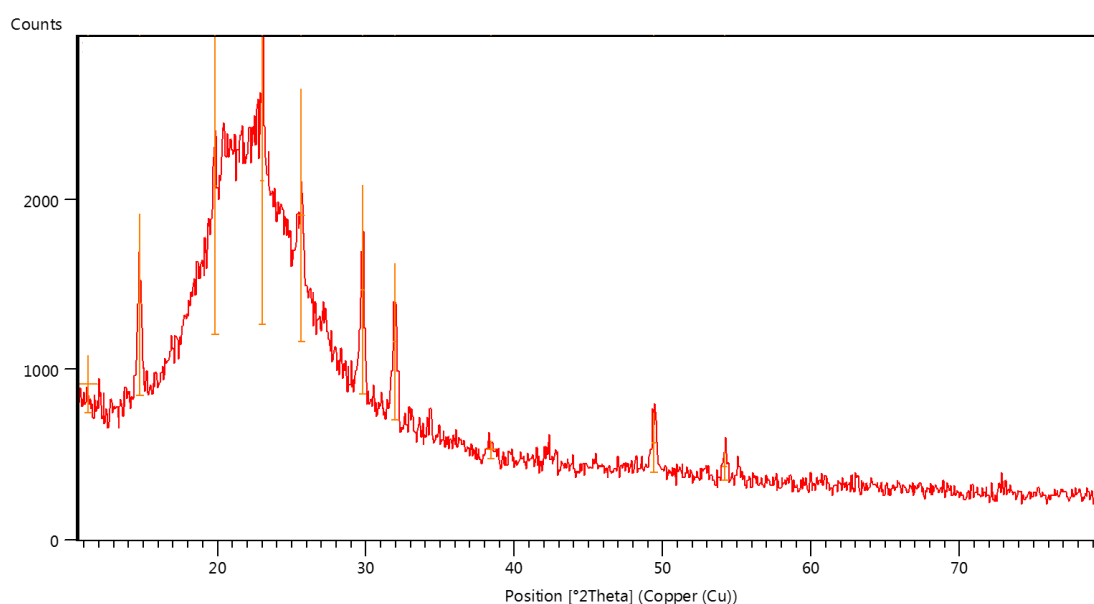


Fig. 6. The XRD pattern of SPBDS.

Table 1. The XRD data of SPBDS

2θ (°)	FWHM (°)	Interplanar distance (nm)	Rel. Int. (%)	Particle size (nm)
11.3243	1.1808	0.7814	16.10	6.77
14.7776	0.1968	0.5995	51.14	40.73
19.7969	0.1968	0.4485	87.70	41.01
22.9908	0.1968	0.3868	100.00	41.22
25.6197	0.4920	0.3477	70.88	16.57
29.7490	0.1968	0.3003	58.69	41.80
31.9345	0.2460	0.2803	44.05	33.62
38.4054	0.5904	0.2344	4.91	14.26
49.4446	0.3936	0.1843	16.53	22.24
54.2140	0.2952	0.1692	8.18	30.26

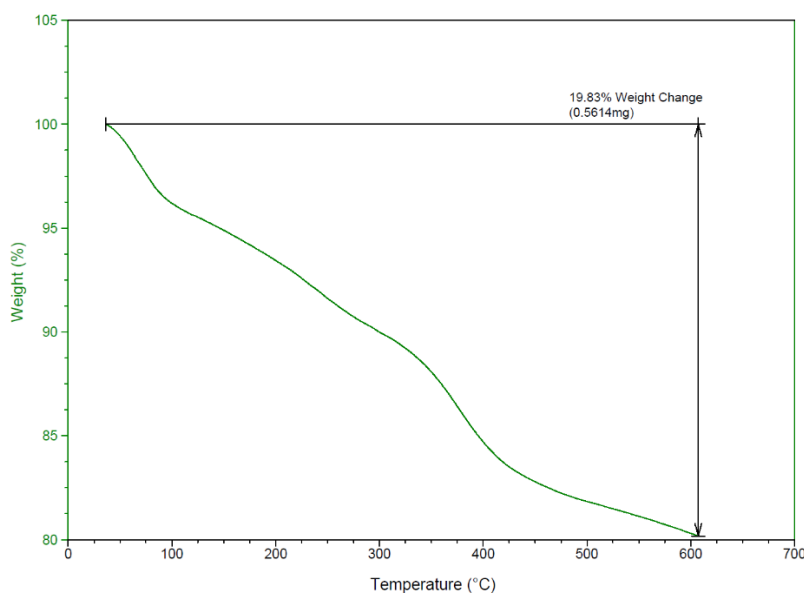
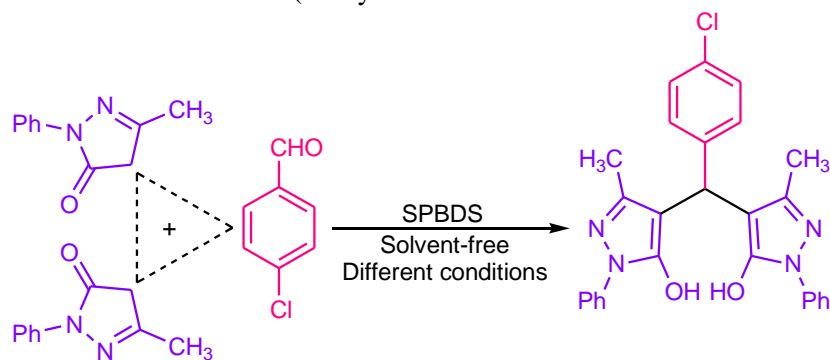


Fig. 7. The TG diagram of SPBDS.

3.2. Application of SPBDS for the construction of bis(pyrazolyl)methanes

The Catalytic applicability of SPBDS was tested for the construction of bis(pyrazolyl)methanes. To perform this test, a model reaction was opted {the condensation of 3-methyl-1-phenyl-1*H*-pyrazol-5(4*H*)-one (1 mmol) with 4-chlorobenzaldehyde (0.5 mmol) (**Scheme 2**)}, and effect of two momentous reaction variable (catalyst

loading and temperature) was studied on the reaction; the main results are reported in **Table 2**. Considering the results, the optimized catalyst loading was 0.030 g, and the optimal temperature in which the reaction effectively progressed was 80 °C (entry 3 of **Table 2**). Enhancement of the catalyst loading up to 0.035 g and the temperature up to 85 °C didn't improve the reaction times and yields (entries 4 and 6 of **Table 2**).



Scheme 2. The model reaction

Table 2. The results of optimizing the reaction conditions

Entry	Amount of SPBDS (g)	Temp. (°C)	Time (min)	Yield (%)
1	0.020	80	30	91
2	0.025	80	15	94
3	0.030	80	15	98 ^a
4	0.035	80	15	98 ^a
5	0.030	70	25	92
6	0.030	85	15	98 ^a

^aThe reaction was completed.

In continuing, the scope and efficacy of SPBDS for the construction of bis(pyrazolyl)methanes were explored by extending the reaction to a number of substituted aryl aldehydes; the results are illustrated in **Table 3**. Considering the data of **Table 3**, it can be said that the substituent type (halogen, electron-releasing, or electron-withdrawing) and its position (para, meta, or ortho) had no significant influence on the reaction times and yields, and the reaction was effectually carried out in all cases. This study corroborated the high effectiveness and extensive scope of SPBDS to catalyze this reaction. As demonstrated in the reaction mechanism (**Scheme 3**), H_2PO_4^- of SPBDS catalyzes the construction of bis(pyrazolyl)methanes *via* activating the electrophiles (by its acidic hydrogen) and the nucleophiles (by its negative oxygen as a weak base) in steps 1 and 3, helping removal of H_2O in step 2, and assisting tautomerization in steps 1, 3 and 4. The mechanism was suggested based on the literature reports [35, 44]. The construction of bis(pyrazolyl)methane **1b** was picked out to study the recoverability and reusability of SPBDS; it was recovered according to the protocol given in the experimental section. **Fig. 8** demonstrates the reusability results; SPBDS was

reusable for nine times without a significant decrement in its catalytic performance.

A Comparison of the reaction conditions and the results of SPBDS with those of some reported catalysts in the construction of bis(pyrazolyl)methanes **1a** and **1b** is illustrated in **Table 4**. This comparison confirmed the superiority of our catalyst with respect to these reported catalysts in one or more of these factors: the reaction conditions (solvent-free versus the usage of organic solvent), temperature, time, and yield. The other benefit of our catalyst was excellent reusability; e.g., SPBDS was reusable nine times without significant diminishing in its catalytic performance (**Fig. 8**), but BPHCSF (our recently reported catalyst) was reusable three times without important decrement in catalytic activity (this ability was decreased when reused for the fourth time).

4. Conclusions

We have fabricated 1-(Si-pr)-[4,4'-bipyridine]-1,1'-dium dihydrogen phosphate anchored to nano-silica as a novel organic-inorganic hybrid nanocatalyst and successfully applied it for the construction of bis(pyrazolyl)methanes. Excellent yields, short reaction

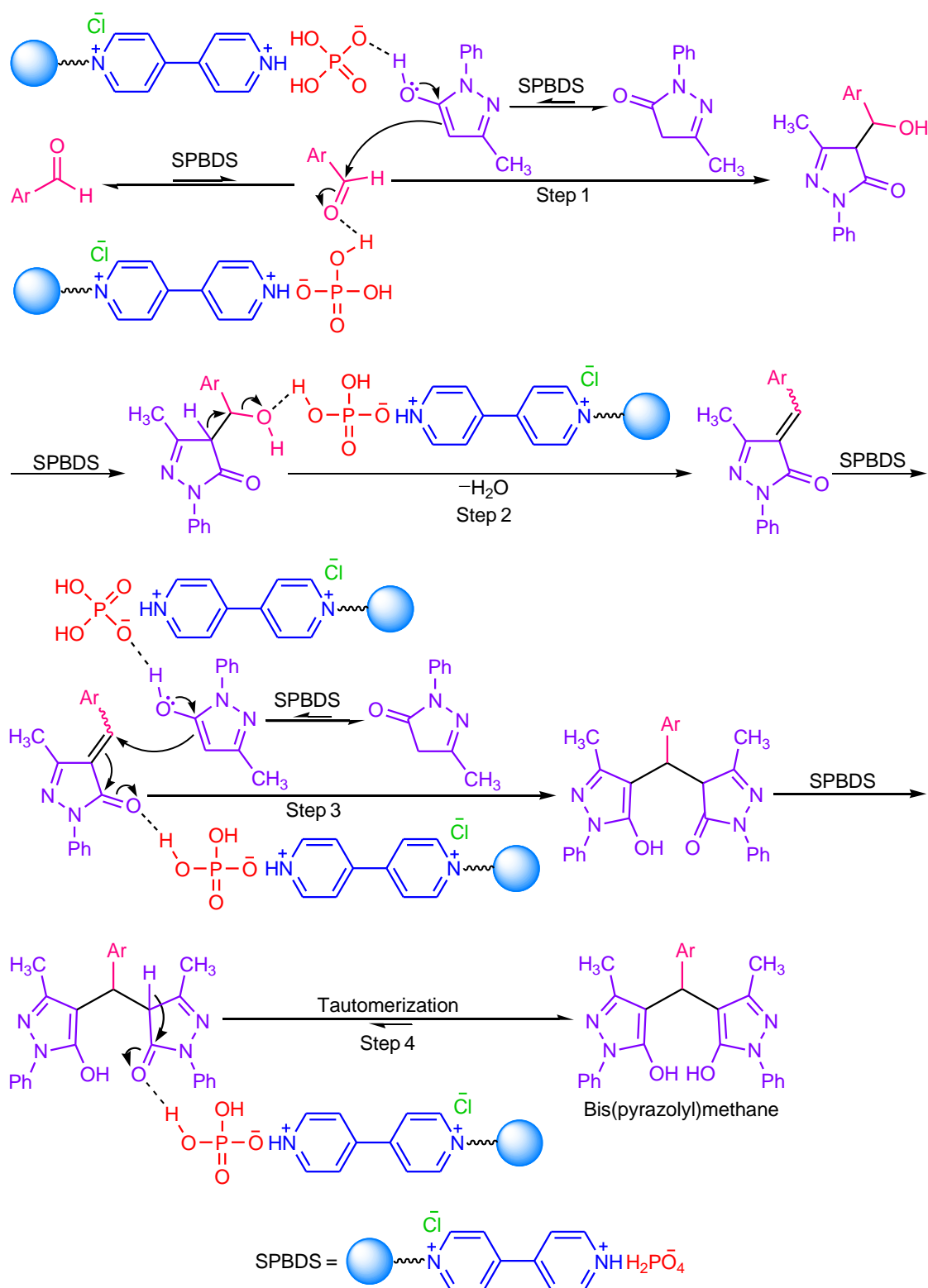
Table 3. The construction of bis(pyrazolyl)methanes using SPBDS



Product No.	Ar	Time (min)	Yield ^a (%)	M.p. (°C) [lit.]
1a	C ₆ H ₅	15	97	170-172 (170-172) [35]
1b	4-ClC ₆ H ₄	15	98 ^b	215-217 (216-218) [37]
1c	2-ClC ₆ H ₄	15	93	236-238 (234-236) [42]
1d	4-CH ₃ C ₆ H ₄	15	97 ^b	201-203 (202-203) [38]
1e	4-CH ₃ OC ₆ H ₄	15	96	171-173 (173-175) [35]
1f	4-PhCH ₂ OC ₆ H ₄	15	98 ^b	213-215 (210-212) [40]
1g	4-HOC ₆ H ₄	20	92	150-152 (153-156) [35]
1h	4-(CH ₃) ₂ NC ₆ H ₄	20	87	184-186 (180-182) [45]
1i	3-O ₂ NC ₆ H ₄	15	98 ^b	152-154 (150-152) [37]
1j	2-O ₂ NC ₆ H ₄	15	98 ^b	224-226 (221-223) [42]

^aIsolated yield.

^bThe reaction was completed.



Scheme 3. The reaction mechanism.

times, generality, excellent reusability, simplicity, use of solvent-free conditions, and good compliance with green chemistry principles are benefits of this protocol.

Acknowledgements

The authors are grateful from Payame Noor University for the support of this work.

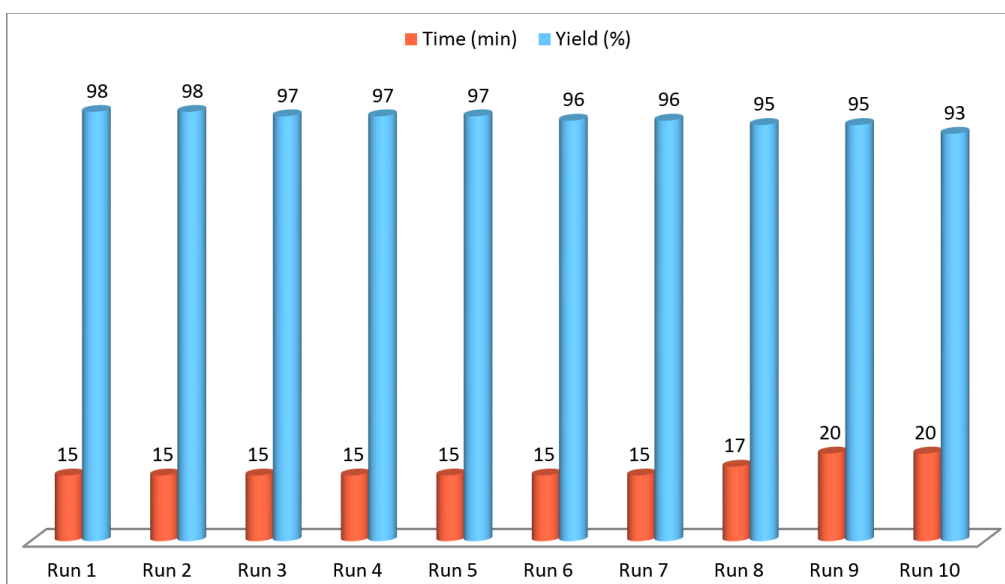


Fig. 8. The results on reusability of SPBDS.

Table 4. Comparative study of the reaction conditions and the results of SPBDS with those of the reported catalysts in the synthesis of compounds **1a** and **1b**

Catalyst	Conditions	Time (min) of products 1a/1b	Yield (%) of products 1a/1b	Ref.
SPBDS	Solvent-free, 80 °C	15/15	97/98	-
SBA-15@Tromethamine-Pr	CH ₃ CN, reflux	15/25	93/97	[35]
Boehmite nanoparticles	Solvent-free, 80 °C	10/10	90/95	[36]
Catalyst-free	Ethylene glycol, 90 °C	60/90	80/91	[37]
Ni-guanidine@MCM-41	CH ₃ CN, 80 °C	30/25	92/90	[38]
BPHCSF ^a	Solvent-free, 70 °C	15/15	96/97	[39]
[Sipmim]HSO ₄ ^b	EtOH, reflux	120/60	89/90	[40]
Humic acid	Solvent-free, 100-130 °C	30/- ^c	90/- ^c	[41]
Nano-Fe ₃ O ₄	Solvent-free, 70 °C	7/3	90/87	[42]
Chitosan-SO ₃ H	Solvent-free, 70 °C	25/15	93/96	[43]
Zirconium@guanine@MCM-41	EtOH, reflux	20/15	99/98	[44]

^a4,4'-Bipyridin-1-ium hydrogen sulfate grafted on chloropropyl functionalized silica gel-nano-Fe₃O₄.

^bN-(3-Silicapropyl)-N-methyl imidazolium hydrogen sulfate.

^cIn the research, this compound has not been produced.

References

- [1] V.P. Ananikov, *Nanomaterials* 9 (2019) 1-6.
- [2] F. Ghorbanipour, S. Mirani Nezhad, S.A. Pourmousavi, E. Nazarzadeh Zare, G. Heidari, *Inorg. Chem. Commun.* 147 (2023) 110271.
- [3] P. Rana, R. Dixit, S. Sharma, S. Dutta, S. Yadav, B. Arora, B. Kaushik, M.B. Gawande, R.K. Sharma, *Nanoscale* 15 (2023) 3482-3495.
- [4] M. Barazandehdoust, M. Mamaghani, H. Kefayati, *Iran. J. Catal.* 12 (2022) 417-429.
- [5] A. Zare, M. Dianat, M.M. Eskandari, *New J. Chem.* 44 (2020) 4736-4743.
- [6] S. Rezayati, F. Kalantari, A. Ramazani, S. Sajjadifar, H. Aghahosseini, A. Rezaei, *Inorg. Chem.* 61 (2022) 992-1010.
- [7] S. Sharifi Sharifabad, B.B.F. Mirjalili, A. Bamoniri, *Iran. J. Catal.* 12 (2022) 365-372.

- [8] A. Zare, J. Atashrooz, M.M. Eskandari, Res. Chem. Intermed. 47 (2021) 1349-1358.
- [9] M. Barzegar, A. Zare, A. Ghobadpoor, M. Dianat, Iran. J. Catal. 12 (2022) 13-24.
- [10] G. Mohammadi Ziarani, Z. Kheilkordi, F. Mohajer, A. Badieli, R. Luque, RSC Adv. 11 (2021) 17456-17477.
- [11] A. Shamaei, B. Mahmoudi, M. Kazemnejadi, M.A. Nasserli, Appl. Organomet. Chem. 34 (2020) e5997.
- [12] G. Pan, T.-t. Jia, Q.-x. Huang, Y.-y. Qiu, J. Xu, P.-h. Yin, T. Liu, Colloids Surf. B: Biointerfaces 159 (2017) 375-385.
- [13] M.N. Hasan, M.S. Salman, M.M. Hasan, K.T. Kubra, M.C. Sheikh, A.I. Rehan, A.I. Rasee, M.E. Awual, R.M. Waliullah, M.S. Hossain, A. Islam, S. Khandaker, A.K.D. Alsukaibi, H.M. Alshammari, M.R. Awual, J. Mol. Struct. 1276 (2023) 134795.
- [14] L. Sun, T. Liu, H. Li, L. Yang, L. Meng, Q. Lu, J. Long, ACS Appl. Mater. Interfaces 7 (2015) 4990-4997.
- [15] R. Mizuta, F. Inoue, Y. Sasaki, S.-i. Sawada, K. Akiyoshi, Small 19 (2023) 2206153.
- [16] S. Jamalpour, M. Ghahramani, S.R. Ghaffarian, M. Javanbakht, Polymer 228 (2021) 123924.
- [17] J.-Y. Mao, L. Hu, S.-R. Zhang, Y. Ren, J.-Q. Yang, L. Zhou, Y.-J. Zeng, Y. Zhou, S.-T. Han, J. Mater. Chem. C 7 (2019) 48-59.
- [18] F. Farbod, M. Mazloun-Ardakani, M. Abdollahi-Alibeik, A. Mirvakili, Z. Ramazani, Int. J. Hydrog. Energy 47 (2022) 9864-9875.
- [19] P. Huang, Y. Chen, H. Lin, L. Yu, L. Zhang, L. Wang, Y. Zhu, J. Shi, Biomaterials 125 (2017) 23-37.
- [20] F. Ghorbani, S.A. Pourmousavi, Iran. J. Catal. 12 (2022), 139-157.
- [21] F. Tamaddon, S.E. Tadayonfar, J. Mol. Liq. 280 (2019) 71-78.
- [22] J. Atashrooz, A. Zare, Iran. J. Catal. 12 (2022) 127-137.
- [23] A. Zare, F. Monfared, S.S. Sajadikhah, Appl. Organomet. Chem. 34 (2020) e6046.
- [24] A. Ansari, A. Ali, M. Asif, Shamsuzzaman, New J. Chem. 41 (2017) 16-41.
- [25] S. Mert, R. Kasimogullari, T. Ica, F. Colak, A. Altun, S. Ok, Eur. J. Med. Chem. 78 (2014) 86-96.
- [26] P.S. Farag, A.M. AboulMagd, M.M. Hemdan, A.I. Hassaballah, Bioorg. Chem. 130 (2023) 106231.
- [27] V.L.M. Silva, J. Elguero, A.M.S. Silva, Eur. J. Med. Chem. 156 (2018) 394-429.
- [28] C.B. Vicentini, C. Romagnoli, E. Andreotti, D. Mares, J. Agric. Food Chem. 55 (2007) 10331-10338.
- [29] Z. Xu, C. Gao, Q.-C. Ren, X.-F. Song, L.-S. Feng, Z.-S. Lv, Eur. J. Med. Chem. 139 (2017) 429-440.
- [30] J. Firdaus, N. Siddiqui, O. Alam, A. Manaihiya, K. Chandra, Arch. Pharm. 356 (2023) e2200421.
- [31] A. Tigreros, J. Portilla, RSC Adv. 10 (2020) 19693-19712.
- [32] K. Wei, S. Lyu, Y. Liu, M. Kang, P. Liu, X. Yang, M. Pei, G. Zhang, New J. Chem. 47 (2023) 751-757.
- [33] H. Chahmout, M. Ouakki, S. Sibous, M. Galai, N. Arrousse, E. Ech-chihbi, Z. Benzekri, S. Boukhris, A. Souizi, M. Cherkaoui, Inorg. Chem. Commun. 147 (2023) 110150.
- [34] M. Cherfi, T. Harit, F. Malek, J. Incl. Phenom. Macrocycl. Chem. 103 (2023) 63-70.
- [35] H. Aghavandi, A. Ghorbani-Choghamarani, M. Mohammadi, Polycycl. Aromat. Compd. 43 (2023) in press, doi: 10.1080/10406638.2022.2147202.
- [36] M. Bakherad, A. Keivanloo, A.H. Amin, R. Doosti, Z. Aghayan, J. Appl. Chem. 11 (2017) 31-37.
- [37] S.S. Kauthale, S.U. Tekale, K.M. Jadhav, R.P. Pawar, Mol. Divers. 20 (2016) 763-770.
- [38] H. Filian, A. Ghorbani-Choghamarani, E. Tahanpesar, J. Iran. Chem. Soc. 16 (2019) 2673-2681.
- [39] E. Jazinizadeh, A. Zare, S.S. Sajadikhah, M. Barzegar, A. Kohzadian, Res. Chem. Intermed. 48 (2022) 2059-2075.
- [40] M. Baghernejad, K. Niknam, Int. J. Chem. 4 (2012) 52-60.
- [41] B. Mitra, P. Ghosh, ChemistrySelect 6 (2021) 68-81.
- [42] A. Zare, F. Abi, V. Khakyzadeh, A. R. Moosavi-Zare, A. Hasaninejad, M. Zarei, Iran. J. Catal. 5 (2015) 311-320.
- [43] P.G. Patil, S. Sehlangia, D.H. More, Synth. Commun. 50 (2020) 1696-1711.
- [44] M. Nikoorazm, M. Mohammadi, M. Khanmoradi, Appl. Organomet. Chem. 34 (2020) e5704.
- [45] P.S. Mahajan, M.D. Nikam, V. Khedkar, P. Jha, P.V. Badadhe, C.H. Gill, J. Heterocycl. Chem. 54 (2017) 1109-1120.